Structural and Electronic Properties of Nanostructured HAlO

Yi Dong,[†,§] Markus Burkhart,[‡,∥] Michael Veith,[‡,⊥] and Michael Springborg*[,†]

Departments of Physical and Theoretical Chemistry and of Inorganic Chemistry, University of Saarland, Postfach 15 11 50, D-66041 Saarbrücken, Germany

Received: July 18, 2005; In Final Form: October 3, 2005

The results of a theoretical study of the nanostructured ternary compound HAlO are presented. We have considered isolated $(HAlO)_n$ clusters, the interactions between two such clusters, and two-dimensional layers of HAlO. In many of the calculations we used a parametrized density-functional tight-binding method in the calculation of the electronic properties for a given structure, combined with two different unbiased approaches, i.e., an "Aufbau" and a genetic-algorithm method, for optimizing the structure for clusters with n up to 26. The results for the isolated clusters are analyzed by means of similarity, stability, and shape parameters. Isolated structures with n up to 6 were also studied intensively with pure DFT methods.

I. Introduction

Theoretical studies on the structural and electronic properties of materials continue to constitute a useful complement to experimental studies, and often the combination of the two approaches gives more information than each of them separately could have contributed. In this work we shall present results of such a study for HAlO with, however, the main emphasis on the theoretical results, although we repeatedly shall make mention of experimental results.

The ternary compound HAlO is an interesting material that can be used as a substrate for organized structures of organic materials, but only little is known about its precise structure. Here, we shall show that theoretical studies can give useful information that ultimately turns out to extend and support the experimental information about it.

HAlO can be prepared either by CVD (chemical vapor deposition) at low temperatures as a thin glassy layer using the precursor bis(*tert*-butoxyalane), $[AlH_2(OtBu)]_2$, and various metals as target substrates,[1,2] or as an amorphous powdered nanostructured material (with considerable content of bymaterial) by the reaction of different methylsiloxanes with the alane $H_3Al{\cdot}NMe_3$ in either ether or aromatic solvents under mild conditions.[3,4] The different preparation routes lead to materials that have similar infrared (IR) spectra, showing a distinctive absorption for the ν(Al—H) stretching mode at 1925 cm^{-1} (layer compound) and 1895−1929 cm^{-1} (powder compound), respectively. Using angle-dependent reflection IR spectroscopy for the layer, a shoulder at 1670 cm^{-1} becomes more prominent when the angle is decreased. This feature can be ascribed to bridging Al—H···Al entities.[6,7] Annealing both layer and powder compound causes the hydride band in the IR spectrum to decrease in intensity. Furthermore, $^{27}Al\{^1H\}$ MAS NMR spectra show resonances for sixfold, fivefold, and fourfold (at 6, 30 and 58 ppm, respectively) coordinated aluminum species; XPS analysis of an HAlO film is consistent with these results.[1,2]

The purpose of the present work is to obtain further information on HAlO by considering both finite clusters and infinite, periodic layers and ultimately present a proposal for the structure of the HAlO compounds.

We studied theoretically the structural properties of the $(HAlO)_n$ clusters with n up to 26 using a density-functional-theory tight-binding method. This method can give the electronic properties for a given structure as well as determine a structure of a local total-energy minimum once an initial structure has been chosen. However, the method is not directly able to determine the structure of the global total-energy minimum. To search for that for the $(HAlO)_n$ clusters, we have used two unbiased approaches, i.e., a method we have called the "Aufbau" method as well as genetic algorithms.

To verify the results of these methods, we also performed pure DFT calculations on smaller $(HAlO)_n$ units with $n = 1$, 2, 3, 4, and 6. For each n we considered several different isomers, as well as the calculation of their vibrational spectra.

Since the experimentally produced nanostructured material is extended, it must contain nanostructures in close contact. Therefore, we also studied the interactions between pairs of optimized $(HAlO)_{n_1}$ and $(HAlO)_{n_2}$ clusters for different values of n_1 and n_2. Finally, the fact that HAlO can be synthesized as a layer compound made us study infinite, periodic, two-dimensional layers of HAlO, too.

The paper is organized as follows. In section II we describe details of the calculational methods that are used to study the HAlO clusters and layers. Subsequently, the results for isolated clusters are presented in section III, and in that section we also discuss the interaction between two clusters, as well as the properties of two-dimensional layers of HAlO. A brief summary of our conclusions is given in section IV. Finally, for the sake of completeness we mention that a brief account of parts of the present study was published previously.[5]

II. Computation Methods

A. Parametrized Density-Functional Method. Many of the calculations of the electronic properties for a given structure were performed using the parametrized tight-binding density-functional method of Seifert et al.[8−10] According to this method, the relative total energy of a given compound with a chosen

* To whom correspondence should be addressed. E-mail: m.springborg@mx.uni-saarland.de.
† Department of Physical and Theoretical Chemistry.
‡ Department of Inorganic Chemistry.
§ E-mail: y.dong@mx.uni-saarland.de.
∥ E-mail: m.burkhart@mx.uni-saarland.de.
⊥ E-mail: veith@mx.uni-saarland.de.

10.1021/jp0539369 CCC: $30.25
Published on Web 11/12/2005

structure is written as the difference in the orbital energies of the compound minus those of the isolated atoms, i.e., as

$$\sum_i \epsilon_i - \sum_m \sum_i \epsilon_{mi} \quad (1)$$

(with m being an atom index and i an orbital index), augmented with pair potentials,

$$\sum_{m_1 \neq m_2} U_{m_1,m_2}(|\vec{R}_{m_1} - \vec{R}_{m_2}|) \quad (2)$$

(with $\vec{R}_m$ being the position of the mth atom).

In calculating the orbital energies, we need the Hamilton matrix elements $\langle \chi_{m_1 n_1} | \hat{H} | \chi_{m_2 n_2} \rangle$ and the overlap matrix elements $\langle \chi_{m_1 n_1} | \chi_{m_2 n_2} \rangle$. Here, χ_{mn} is the nth atomic orbital of the mth atom. The Hamilton operator contains the kinetic-energy operator as well as the potential. The latter is approximated as a superposition of the potentials of the isolated atoms,

$$V(\vec{r}) = \sum_m V_m(|\vec{r} - \vec{R}_m|) \quad (3)$$

and subsequently we assume that the matrix element $\langle \chi_{m_1 n_1} | V_m | \chi_{m_2 n_2} \rangle$ vanishes unless at least one of the atoms m_1 and m_2 equals m. Finally, the pair potentials U_{m_1,m_2} are obtained by requiring that the total-energy curves from parameter-free density-functional calculations on the diatomics are accurately reproduced. With these approximations, all relevant information on the above-mentioned matrix elements can be extracted from calculations on isolated two-atomic systems, in our case on H_2, HAl, HO, Al_2, AlO, and O_2.

B. Unbiased Structure Optimizations. With the method above we can calculate the total energy of a given structure, and by calculating also the forces acting on the atoms, i.e., the derivatives of the total energy with respect to nuclear coordinates, also the structure of a local total-energy minimum can be identified. To search for the structure of the global total-energy minimum for the isolated $(HAlO)_n$ clusters, we have used two different, unbiased approaches, i.e., our own Aufbau method as well as a method based on genetic algorithms. The only information we use is that HAlO is stoichiometric.[1,2] With our Aufbau method, that is closely related to our "Aufbau/Abbau" method that we have used in optimizing the structure of large metal clusters,[11] we start out optimizing the structure of a single HAlO molecule (i.e., $n = 1$) by choosing the structure of the lowest total energy from a very large number of calculations on randomly constructed structures that were allowed to relax to their closest total-energy minimum. Subsequently, we only assume that the structure of the cluster with $n + 1$ units can be obtained by adding one Al, one O, and one H atom to the cluster with n units. Thus, out of very many calculations where we randomly add those three atoms to the optimized structure of the cluster with n units (imposing only the constraints that the extra atoms should not be too close to any other atom or too far from all the other ones, and subsequently allowed to relax) we obtain an optimized structure of the system with $n + 1$ units. This is repeated starting from $n = 1$ up to, in our case, $n = 26$.

The resulting cluster of such a calculation is not with absolute certainty that of the global total-energy minimum but, hopefully, a very good approximation to it.

Our other approach is based on the so-called genetic algorithms, which in turn are based on the principles of natural evolution and are, therefore, also called evolutionary algorithms.[12,13] We found that it provides an efficient tool for global geometry optimizations. Our version of the genetic algorithms is as follows. Suppose that we have optimized the structure of the cluster with n units. From this structure we construct a first generation consisting of M independent clusters for the $(n + 1)$-unit system by randomly adding one Al, one O, and one H atom and letting these structures relax to their nearest total-energy minima. Subsequently, a new set of clusters is constructed by cutting each of the original ones randomly into two parts that are interchanged (under the constraints mentioned above) and, afterward, allowed to relax. Out of the total set of $2M$ structures, the M ones of the lowest total energy are kept as the next generation. This procedure is repeated until the lowest total energy is unchanged for a large number of generations.

By comparing the results from the two sets of (independent) calculations, i.e., using the Aufbau method and the genetic algorithms, we have a possibility to check the reliability of each approach.

C. Pure DFT Calculations. In addition to the calculations using the Aufbau method and the genetic algorithms, we performed calculations using Ahlrichs' program system TURBOMOLE.[14] All calculations used pure DFT with the Becke−Perdew functional,[15,16,17,18] employing SV(P) basis sets.[19] The Coulomb terms were treated by the RI-J approximation to speed up computation time for the geometry optimizations (*ri*BP/SV(P)).[20,21]

We studied very many structures of $(HAlO)_n$ with $n = 1$, 2, 3, 4, and 6. Here, starting from "reasonable" starting geometries, relaxed structures were obtained and, subsequently, analyzed. This gave 2, 5, 7, 8, and 28 different structures for $n = 1$, 2, 3, 4, and 6, respectively.

D. Interacting Clusters and Layers. The material HAlO is nanostructured in the powder form and glasslike in the layer form; that is, is believed to consist of smaller "clusters" that, however, are very close to each other. This means that the properties of the individual clusters may to only a smaller extent be recovered for the nanostructured material. To obtain some first insight into the latter, we have also considered the consequences of putting two clusters together. That is. we studied systems consisting of the clusters with n_1 and n_2 units that are placed at positions so close that they interact. Subsequently, they are allowed to relax. We finally select the structure of the lowest total energy from a large set of calculations where we have varied the relative orientations of the two clusters.

Finally, we also studied infinite, periodic, two-dimensional layers of HAlO. Here, we considered both systems containing only one layer as well as systems containing two, covalently bonded, layers. In all cases we constructed an Al−O square lattice from a periodically repeated unit of $N \times N$ Al and O atoms. In one case we considered just a single layer with $N = 8$ and with H atoms added to the Al atoms on only one side of the layer. In another case we considered a single layer with $N = 6$ but with the H atoms added to the Al atoms alternatingly on one or the other side of the layer. Furthermore, we considered two layers placed on top of each other and still with H atoms added to the Al atoms. Here, we had $N = 6$ for the case that the two layers were placed so that Al−Al and O−O bonds between the layers could be formed, whereas we had $N = 4$ for the case when we only had Al−O bonds between the layers. In all cases we varied the lattice constants of the repeated units in order to determine the optimized value, and by varying the value of N, we checked that the results were converged as a function of this parameter.

We add that the calculations on the interacting clusters and on the layers all were performed using the parametrized density-functional method that was described in section IIA.

TABLE 1: Various Parameters Describing the Results of the Optimization of the $(HAlO)_n$ Clusters Using Either the Aufbau or the Genetic-Algorithms Approach[a]

	$n=2$	$n=3$	$n=4$	$n=5$	$n=6$	$n=7$	$n=8$	$n=9$
E_{tot}^{auf}	−4.8238	−4.9275	−5.0673	−5.1190	−5.1892	−5.2367	−5.2892	−5.3377
E_{tot}^{ga}	−4.8238	−4.9275	−5.0673	−5.1190	−5.1914	−5.2376	−5.2908	−5.3396
Δ_r	0.00	0.01	0.00	0.00	0.47	0.44	0.16	0.13
Δ_d	0.00	0.00	0.00	0.00	0.30	0.20	0.075	0.01

[a] n describes the size of the cluster, E_{tot}^{auf} and E_{tot}^{ga} are the calculated total energies (in au per unit) with the two methods, and Δ_r and Δ_d are the two parameters (in au) that are used in quantifying the difference between the structures.

III. Results

First, we optimized the structures of $(HAlO)_n$ clusters with n up to 26 using our Aufbau approach and with n up to 18 using the genetic-algorithms approach. A set of key quantities are shown in Table 1, of which some are introduced in order to compare the results from the two approaches. We define a radial distance $\vec{r}_i$ for each of the $3n$ atoms as

$$r_i = |\vec{R}_i - \vec{R}_0| \tag{4}$$

where $\vec{R}_0$ is the center of the cluster,

$$\vec{R}_0 = \frac{1}{3n}\sum_{i=1}^{3n}\vec{R}_i \tag{5}$$

Subsequently, two parameters are defined as follows

$$\Delta_r = \left[\frac{1}{3n}\sum_{i=1}^{3n}(r_i^{auf} - r_i^{ga})^2\right]^{1/2}$$

$$\Delta_d = \left[\frac{2}{3n(3n-1)}\sum_{i=1}^{3n(3n-1)/2}(d_i^{auf} - d_i^{ga})^2\right]^{1/2} \tag{6}$$

where d_i are the interatomic distances and where we have assumed that r_i and d_i have been sorted in increasing order. Finally, the upper indices "auf" and "ga" refer to the Aufbau and genetic-algorithms approaches, respectively. The parameter approaches 0 if the two structures are very similar. In Table 1 we see that the lowest total energies from the two approaches are very close and, moreover, in both cases show the same tendency that the energy per unit decreases with increasing size of the cluster. Furthermore, the two parameters defined above that quantify the structural differences are also very small. The above analysis gives us strong reasons to suggest that the global total-energy minimum of the $(HAlO)_n$ clusters has been found and also that our two unbiased approaches are reliable.

Further support for our conclusion is obtained from the results of the pure DFT calculations, as shall be discussed below. Using this pure DFT technique, we first studied the HAlO monomers in order to compare with previously published data using SCF and MP3 methods.[22] Our calculations show that for the HAlO monomer the hydroxyde AlOH is more stable than the hydride HAlO, as also found in the SCF and MP3 calculations. For $n \geq 2$ the hydridic species become more stable than the corresponding hydroxides. Comparing the geometries, our bond lengths are slightly longer than those of the previously published results. Maybe not surprising, the structures of the energetically lowest isomers of $(HAlO)_n$ for $n > 2$ as calculated with the parametrized method and as calculated with the parameter-free method are not identical, which may be ascribed to the occurrence of several (meta-)stable structures with a different energetic ordering in the two theoretical approaches. However, as we shall see below, the overall picture that emerges from the calculations with the two different methods is mutually consistent.

As examples of the results of the calculations, we show in Figure 1 optimized structures using the different methods. As exemplified in the figure, it turned out that all optimized $(HAlO)_n$ clusters have a structure where the Al and O atoms form an inner part of the cluster, whereas the H atoms are only found on the surface of the cluster. Moreover, in the inner part of the clusters there are mainly Al−O bonds and essentially no Al−Al or O−O bonds, and on the surface the H atoms are bonded only to Al atoms. Parts of this are illustrated in Figure 4, which shows the radial distances for the different clusters and atoms. The figure contains, for each type of atoms separately, the radial distances for the different values of n. It is very clear that the largest radial distances are found for H atoms and, in addition, that essentially all H atoms always have larger radial distances than the Al and O atoms. On the other hand, the central parts of the clusters are clearly formed by both Al and O atoms.

Experimental results on $(HAlO)_n$ clusters are not available, but derivatives of the type $(RAlO)_n$ (R = bulky organic ligand) have been prepared and the crystal structures of $(RAlO)_4$ (R = C_6H_2-2,4,6-*t*-Bu_3) and $(RAlO)_6$ (R = *t*-Bu) have been determined.[23,24] While the tetrameric unit forms a twisted Al_4O_4 ring, which is due to the special ligand used, $(t\text{-}BuAlO)_6$ has a drum-shaped structure very similar to one of our calculated isomers.[23,24]

Also, the DFT calculations on the smallest cluster give results in support of this general structure. As mentioned above, we considered in total 50 isomers of $(HAlO)_n$ with n = 1, 2, 3, 4, and 6. To extract information from these results, we proceed as follows. First we analyzed the interatomic distances for all 50 structures. It turned out that none possessed O−O or H−H nearest neighbors and that it was relative easy to identify Al−H, Al−O, and O−H bonds as being pairs with an interatomic distance smaller than 2.2, 2.5, and 1.5 Å, respectively. The Al−Al interatomic distances, on the other hand, showed a large spread, and it was not possible to readily identify a cutoff distance below which the Al atoms could be considered as being bonded. In the subsequent analysis we therefore considered two extreme values, 2.5 and 4.1 Å.

Next we studied the total energy per unit as a function of number of A−B bonds per unit, with A and B being H, Al, and O. The results are shown in Figure 2. The results are very scattered, but nevertheless, it is possible to identify certain trends. First, the total energy decreases as the number of Al−O bonds increases. Second, a similar, but much weaker, trend can be identified for the number of Al−Al bonds (here we have used 4.1 Å as our cutoff value, but 2.5 Å gives very similar results). Third, there is a clear preference for structures with one Al−H bond per unit. These observations can be quantified

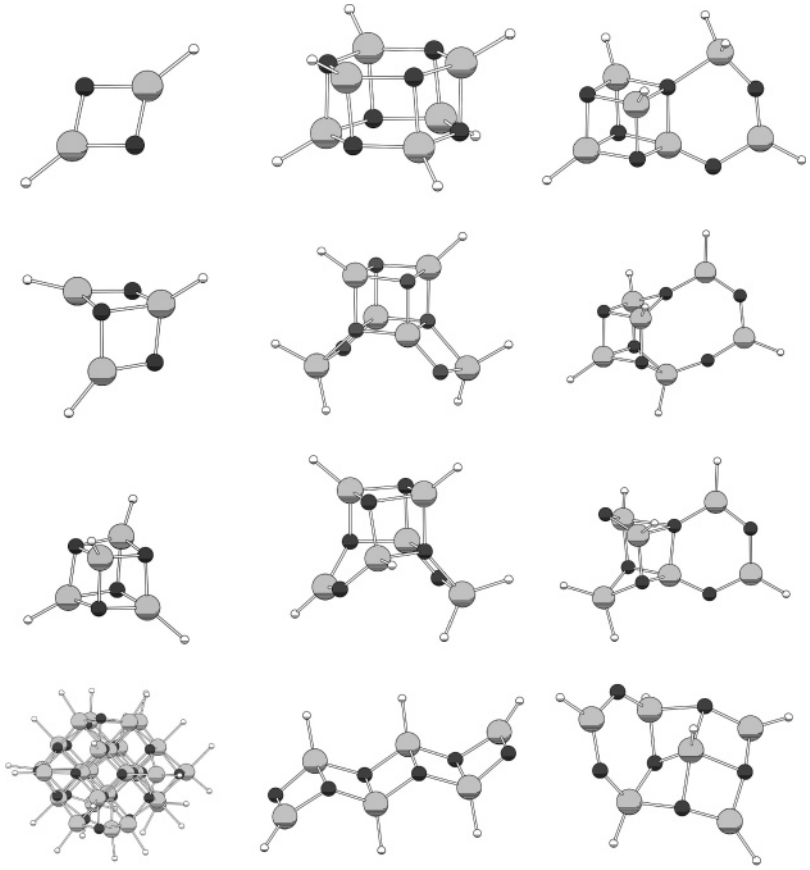

Figure 1. $(HAlO)_n$ structures. The left side shows clusters with $n = 2$, 3, 4, and 26 from DFT-TB calculations using the Aufbau method in the structure optimization (top to bottom). The other structures show different isomers (DFT calculations) for the $(HAlO)_6$ system. Hydrogen, aluminum, and oxygen are represented with small white spheres, large gray spheres, and black spheres, respectively.

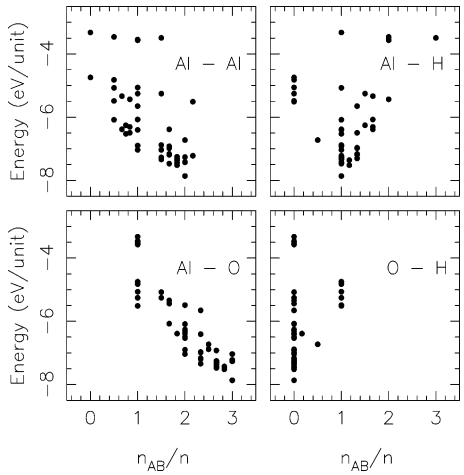

Figure 2. Variation in the total energy per unit as a function of the number of A−B bonds per unit. The results are from the DFT calculations for the $(HAlO)_n$ clusters with $n = 1$, 2, 3, 4, and 6, and the meaning of A and B is given in the panels.

by approximating the total energy of the various $(HAlO)_n$ isomers as

$$E_{tot} \simeq nE_0 + n_{AlAl}E_{AlAl} + n_{AlO}E_{AlO} + n_{AlH}E_{AlH} + n_{OH}E_{OH} \quad (7)$$

A least-squares fit to our 50 DFT results gave $E_{AlAl} = -0.175$ eV (−0.122 eV), $E_{AlO} = -1.000$ eV (−1.170 eV), $E_{AlH} = 0.750$ eV (0.678 eV), and $E_{OH} = 1.119$ eV (0.798 eV), when using 4.1 Å (2.5 Å) as the cutoff distance for Al−Al bonds. These numbers show that Al−O bonds are strongly preferred and that

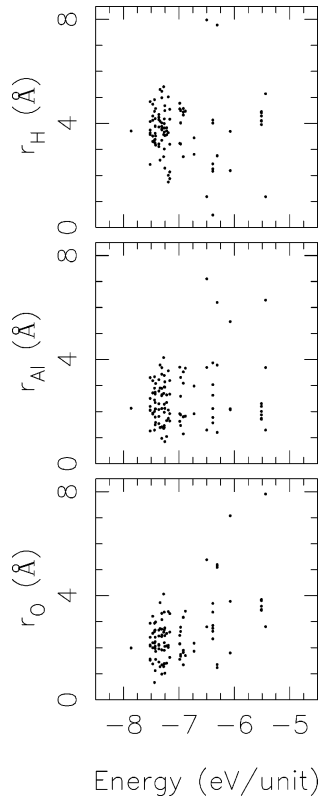

Figure 3. Radial distances for the different smaller clusters as a function of the total energy per unit. The different panels show the different types of atoms. The results are from the DFT calculations for the $(HAlO)_n$ clusters with $n = 6$.

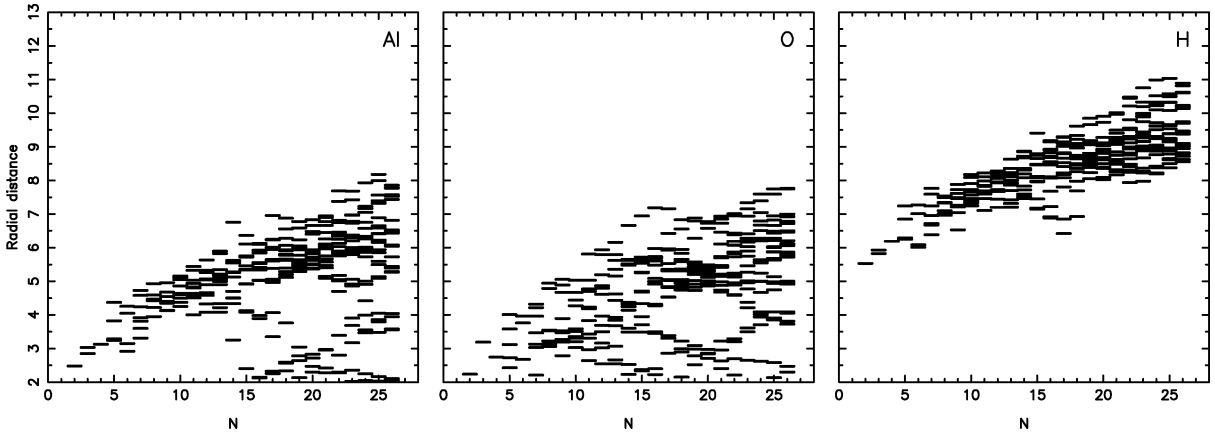

Figure 4. Radial distances (in au) for Al, O, and H atoms, separately, as a function of the size of the cluster n for $(HAlO)_n$ clusters. In each panel, a small horizontal line shows that at least one atom of the corresponding type has that distance to the center of the cluster for a given value of n.

when choosing between adding H to either Al or O, it is energetically preferred to create Al−H bonds. These features are in perfect agreement with the results for the structure optimizations for the larger clusters obtained using the Aufbau or genetic-algorithms method.

For each of the 28 $(HAlO)_6$ clusters, we also calculated the radial distances of the different atoms. Subsequently, we plotted this as a function of the total energy per unit, and we show the results in Figure 3. One should remember that the radial distance for each atom of the smaller clusters is on the average smaller than that of the larger clusters. Therefore, we chose to consider only the clusters of the same size, i.e., $(HAlO)_6$. When comparing the clusters of roughly the lowest total energies, we see that Al and O are those atoms with smaller radial distances, whereas those of hydrogen are larger. For the higher total energies, the radial distances of Al and O show a weak tendency to increase and simultaneously those of H are slightly decreasing. In total, this analysis confirms the tendency for the $(HAlO)_n$ clusters to possess a Al−O core covered with H atoms.

The DFT calculations strongly indicate that the stables hydrides mainly have terminal hydrides. Moreover, it is interesting to observe that when comparing isomers with bridging H atoms with isomers with bridging hydroxy groups, isomers with OH groups usually are more stable than the corresponding isomer with bridging H atoms.

We now return to the larger clusters that were studied with the parametrized density-functional method. Figure 5 shows the smallest interatomic distances for different types of pairs, and in Figure 6 we show the pair correlation functions $g_{AB}(R)$ for the clusters with $n = 2$ and $n = 26$. Here, $g_{AB}(R)$ is the number of A−B pairs with an interatomic distance of R. It is seen that there is a strong preference for Al−O and Al−H nearest-neighbor bonds, both for the small and for the large clusters. For the sake of completeness, we add that the bond lengths for diatomic AlO and AlH are 3.33 au = 1.76 Å and 3.06 au = 1.62 Å, respectively. By analyzing the nearest surroundings of the Al atoms, we find that the coordination number of Al is between 3 and 6 with the value 6 for Al atoms that are in the central part of the clusters. This is in excellent agreement with the NMR data.

The stability of a given cluster can be analyzed through the total energies. Most conveniently, this is done by using the stability function

$$\Delta E_n = E_{tot}(n+1) + E_{tot}(n-1) - 2E_{tot}(n) \qquad (8)$$

This function is shown in Figure 7. It has peaks for particularly stable clusters, i.e., for $n = 4$, 19, and 22. As we shall see below, the cluster for $n = 4$ is highly symmetric and, as shown in Figure 7, also particularly stable.

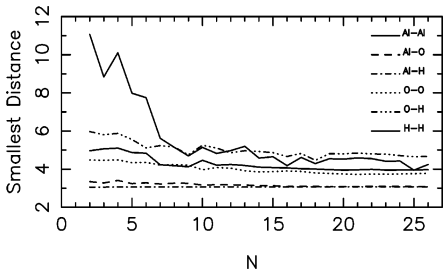

Figure 5. Smallest interatomic A−B distances (in au) for $(HAlO)_n$ clusters for different values of n and different pairs of atoms.

The overall shape of the clusters can be quantified by considering the eigenvalues $I_{\alpha\alpha}$ of the matrix containing the moments of inertia relative to the center of the cluster. The shape of the cluster is roughly spherical if all three eigenvalues are identical, whereas the cluster has a lenslike shape if two eigenvalues are larger than the average eigenvalue, and finally, it has an overall cigarlike shape if two eigenvalues are smaller than the average eigenvalue. This analysis is shown in Figure 8. For a homogeneous sphere of constant density, the eigenvalues scale as $n^{5/3}$ and, therefore, the results of Figure 8 have been scaled with $n^{-5/3}$. In Figure 8 it is seen, as mentioned above, that the cluster with $n = 4$ has spherical shape, whereas lenslike and cigarlike shapes occur for all other clusters studied here.

Our two approaches for structure optimization, i.e., the Aufbau and genetic algorithms, are both based on building up the $(n + 1)$ cluster from the one with n units, suggesting that the structure of the $(n + 1)$ cluster is closely related to that of the n cluster. Also, Figure 8 suggests that the structure is, at least over certain ranges of n, relatively unchanging. We can quantify whether the structure of the cluster with $n + 1$ units is similar to the structure of the cluster with n units as follows. We consider all the n-unit fragments of the $(n + 1)$-unit cluster that can be obtained by removing one H, one Al, and one O atom [i.e., in total we consider $(n + 1)^3$ different fragments]. Subsequently, we calculate and sort all interatomic distances for this fragment $\{R'_{n+1,i}\}$. These are compared with the sorted interatomic distances $\{R_{n,i}\}$ for the n-unit system; that is, we construct

$$\frac{3n(3n-1)}{2}q^2 = \sum_{i=1}^{3n(3n-1)/2} (R'_{n+1,i} - R_{n,i})^2 \qquad (9)$$

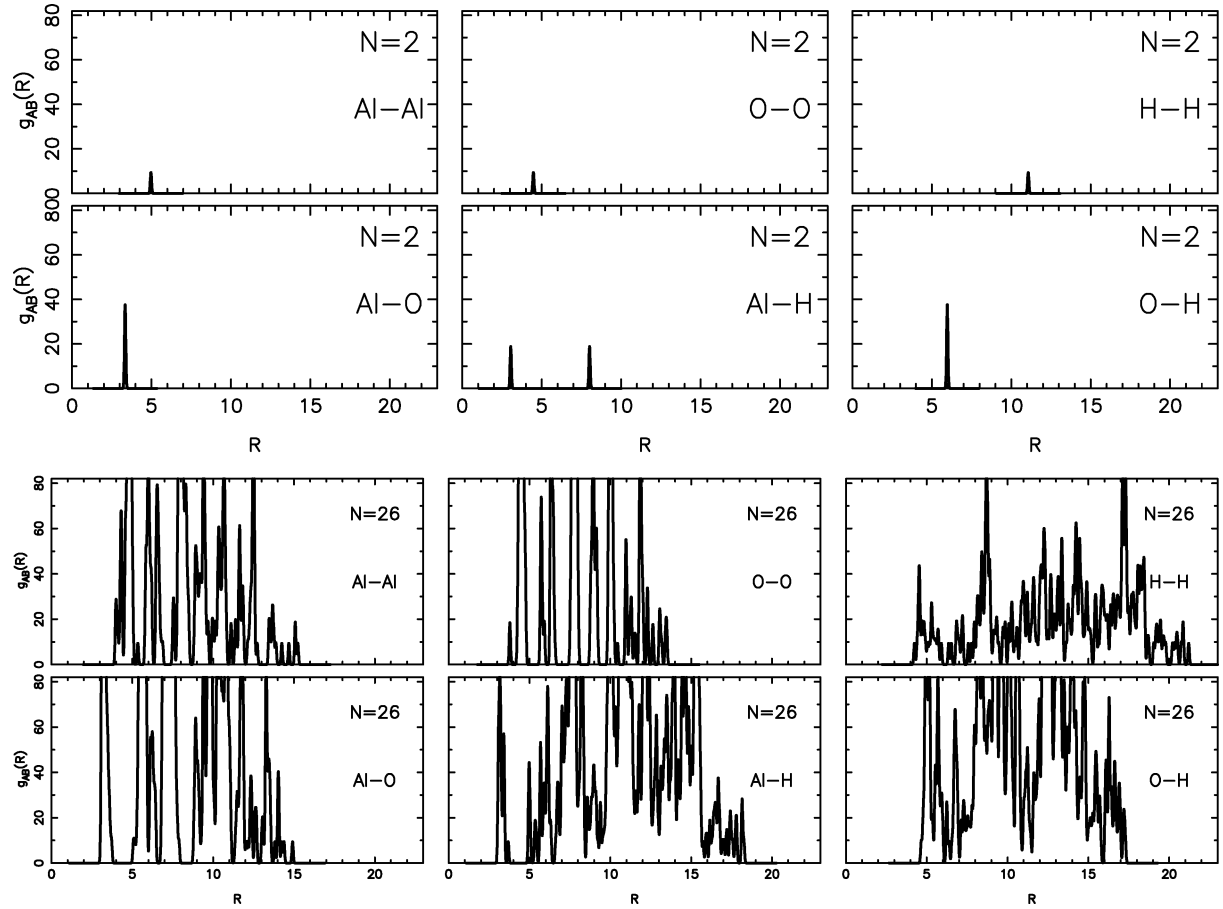

Figure 6. Pair-correlation functions $g_{AB}(R)$ for (upper part) $n = 2$ and (lower part) $n = 26$ with R in au.

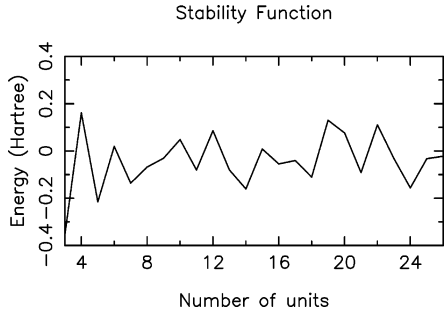

Figure 7. Stability function for $(HAlO)_n$ clusters as a function of n.

Out of the $(n + 1)^3$ values of q, we choose the smallest value of q, i.e., q_{min}, that subsequently defines the similarity function

$$S = \frac{1}{1 + q_{min}/a_0} \tag{10}$$

with a_0 chosen equal to 1 au, S approaches 1 if the $(n + 1)$-unit cluster is very similar to the n-unit cluster plus one unit and 0 for structurally very different systems.

Figure 9 shows this similarity function for the clusters with $n = 2$ to $n = 25$. It is obvious that, for the smaller clusters, the cluster with $n + 1$ units is certainly not similar to the n-unit cluster, and the growth of the clusters is, accordingly, not regular. On the other hand, for the larger clusters, the similarity function approaches 1, although, also for those, significant structural changes occur, as we have also seen through our other structure descriptors.

In discussing the electronic properties of the clusters, we consider solely the largest one of the present study, i.e., the

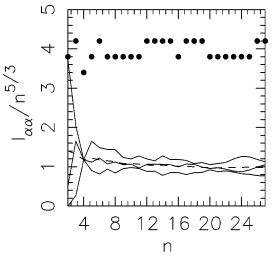

Figure 8. Eigenvalues, $I_{\alpha\alpha}$, of the matrix with the moments of inertia for $(HAlO)_n$ clusters as a function of n. To obtain values of $I_{\alpha\alpha}$ that are roughly independent of n, they have been scaled by $n^{-5/3}$. The marks on the top indicate whether the cluster has an overall spherical shape (lowest row), a cigarlike shape (middle row), or a lenslike shape (upper row). The dashed curve is the average of the three eigenvalues.

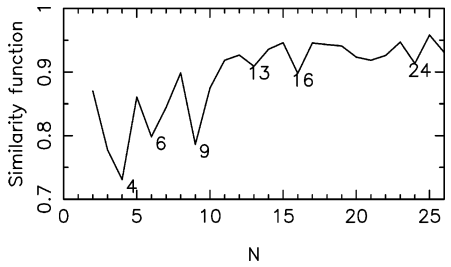

Figure 9. Similarity function for $(HAlO)_n$ clusters as a function of n.

one with $n = 26$. First we show in Figure 10 the radial distributions of the Mulliken *gross* populations; that is, we calculate the *gross* population for each atom separately and depict them subsequently as a function of the radial distance of eq 4. This picture confirms the consensus from above that the H atoms are those with the largest radial distances. Moreover,

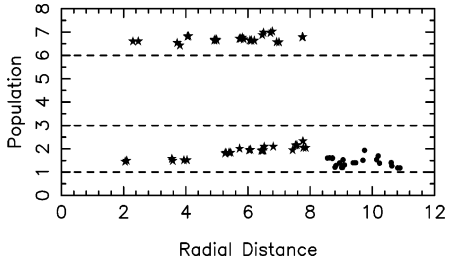

Figure 10. Radial distribution of the Mulliken *gross* populations of the valence electrons for the $(HAlO)_{26}$ cluster. The horizontal dashed lines mark the values for the neutral atoms, i.e., 1, 3, and 6 for H, Al, and O, respectively. Al and O atoms are marked by stars, H atoms are marked by closed circles, and the radial distance is given in au.

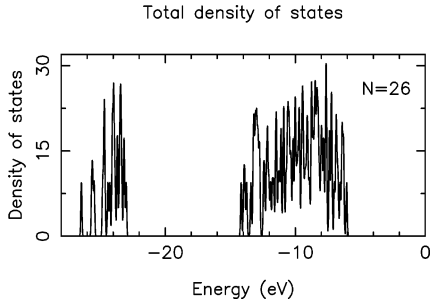

Figure 11. Density of states of the valence orbitals in arbitrary units for the $(HAlO)_{26}$ cluster. It has been obtained from the discrete energy levels upon a broadening with narrow Gaussians. All shown orbitals are occupied, whereas the unoccupied ones appear at positive energies.

it is seen that both O and H atoms receive electrons, whereas the Al atoms donate electrons. For the Al atoms, there seems to be a larger donation of electrons in the innermost parts of the cluster, whereas a similar trend not is observed for the O atoms.

For all geometries that were studied with the DFT method, we also calculated the IR spectrum. Therefore, we can compare the theoretical vibrational bands with those of the layer compound. Figure 15 shows this result. The theoretical spectrum was constructed as the sum of the spectra for the lowest-total-energy structures of $(HAlO)_n$ ($n = 2$, 3, 4, and 6). Except for the shoulder at 1670 cm^{-1}, there is a very good agreement between theory and experiment. The fact that we do not find the shoulder is reasonable, since all minimal structures of our calculations have terminal hydrides, whereas the shoulder may be due to bridging Al−H−Al units, although a final assignment is lacking at the moment.

In Figure 11 we show the density of states of the valence orbitals for the same cluster. This curve is clearly split into two parts, i.e., a low-energy part around −25 eV due to O 2s functions as well as a high-energy part due to Al 3s, 3p, O 2p, and H 1s functions. The unoccupied orbitals appear at positive energies, so that the gap between occupied an unoccupied orbitals is large.

The HAlO clusters form parts of a nanostructured material, so that they may very likely interact with each other. In this context it is an interesting issue whether the H atoms will try to remain outside a central part, as we have observed for the individual, isolated clusters. We decided, therefore, to study the interaction between two clusters by putting two of the previously optimized clusters together. This was done as follows. We placed two clusters of n_1 and n_2 units so close to each other that they would interact. The initial structures were those of the isolated $(HAlO)_{n_1}$ and $(HAlO)_{n_2}$ clusters, and we considered very many relative orientations of the two clusters, out of which we chose the one that led to the lowest total energy after structural relaxation. Table 2 shows the total energies in comparison with those of the optimized clusters with $n = n_1 + n_2$ units. From the table we see that the interacting clusters are more stable than the two separate, noninteracting clusters but clearly less stable than the larger cluster of n units. For the case that the two clusters were brought so close that they interact, before the combined cluster was relaxed, it was found that the hydrogen atoms are placed between the two cores of AlO, but after the combined cluster was relaxed, the hydrogen atoms are only sitting on the surface of the combined cluster. This supports our consensus that clusters with hydrogen sitting on the surface of the clusters are most stable.

Figure 12 illustrates this idea even further. This figure has been obtained as follows. We consider the case of $n_1 = 8$ and $n_2 = 9$ units before and after relaxation. In each case (i.e., before and after relaxation) we calculate the center of the two parts according to eq 5. The line joining these two centers defines the z axis in a cylindrical coordinate system with $z = 0$ being the midpoint between the two centers. Subsequently, we superpose the two coordinate systems in one figure and show the initial and final values of z and the distance to the z axis (denoted d) for each atom separately by joining these points with a straight line. Finally, we depict these lines for each type of atom individually. The stars mark the final positions of the $n_1 = 8$ system whereas the closed circles mark the final positions of the $n_2 = 9$ system. In particular, the H atoms tend to increase d upon relaxation, i.e., to move away from the region between the two clusters. On the other hand, the first of all the O atoms but also to a lesser extent the Al atoms are seeking to fill out the space between the two clusters when they are combined.

Our experimentally synthesized material is a glasslike, amorphous film.[1,2] Moreover, our theoretical findings, i.e., that the H atoms prefer to stay outside an AlO core, which for larger clusters becomes increasingly difficult when requiring that the

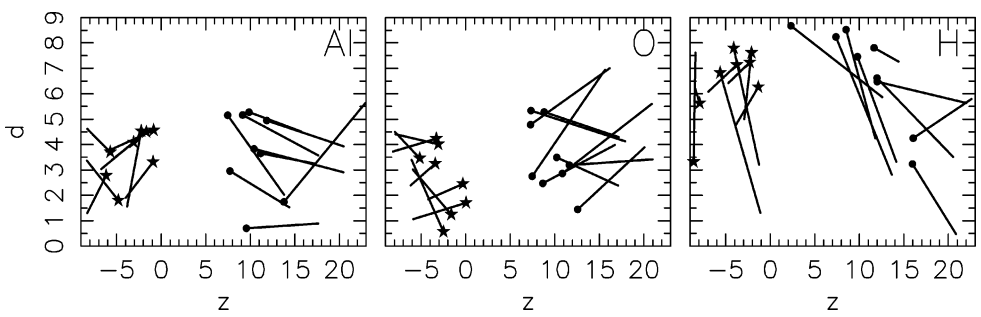

Figure 12. Graphical illustration of the structural relaxations of bringing the $n_1 = 8$ (left part) and $n_2 = 9$ (right part) clusters together. Shown are the relaxations in a cylindrical coordinate system with z and d being the position along the cylindrical axis and the distance from it, respectively, both in au. The three panels show the displacements of the Al, O, and H atoms, individually. For details about the presentation, see the text.

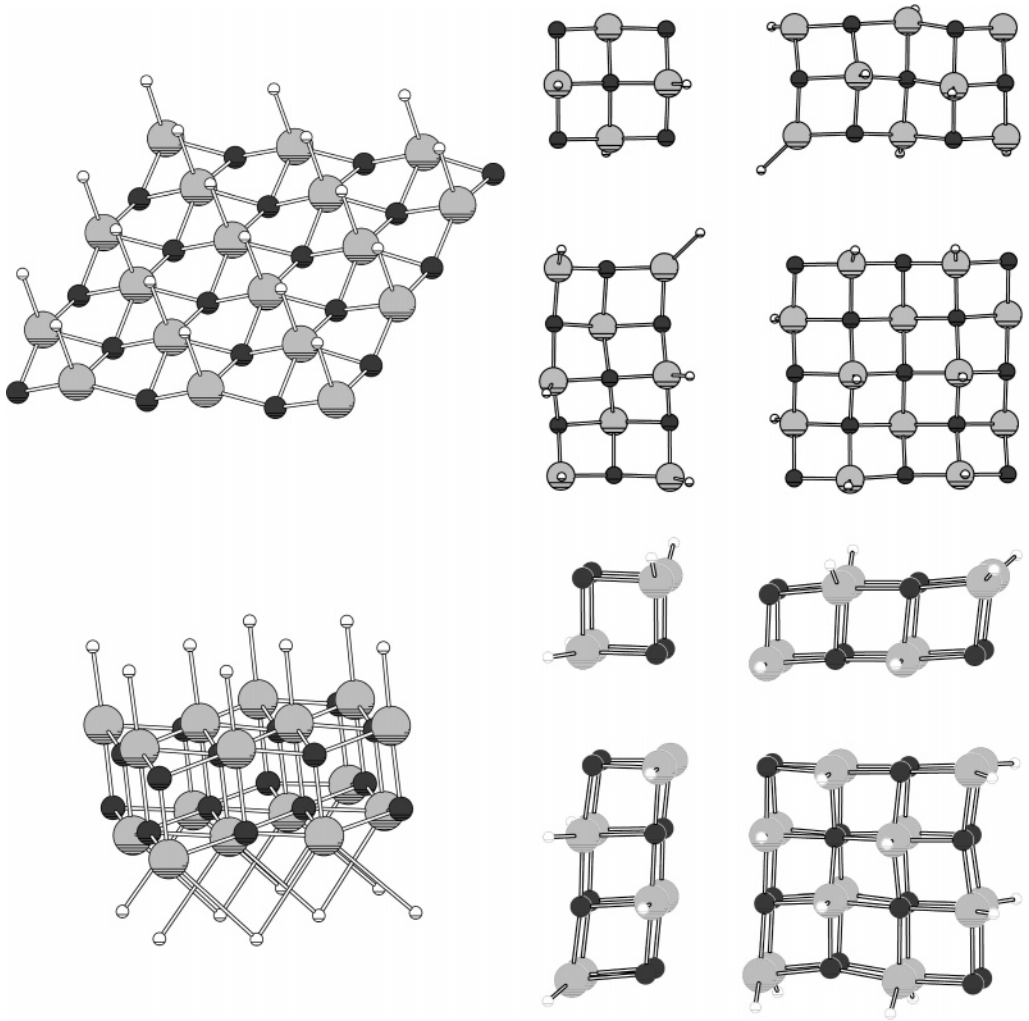

Figure 13. Structure of layers of HAlO for one layer where H atoms are on one side (upper left) or two sides (upper right), as well as for two layers with the Al atoms of one layer above either the O (lower left) or the Al (lower right) atoms of the other layer. We use the same color coding as in Figure 1. Notice that interlayer interactions were not included in the calculations. Moreover, the structures on the right-hand part are seen to split into smaller fragments whose size, however, may be biased by the size of the repeated unit in the calculations.

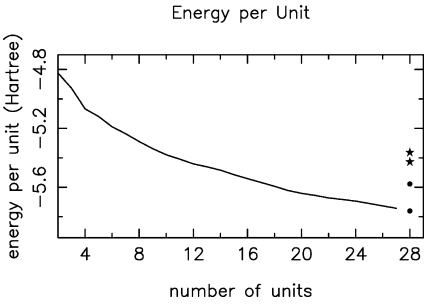

Figure 14. Variation in energy per unit for isolated clusters and for the layers of HAlO. The results for the layers are shown to the right with the one-layer results marked with stars (here, the lowest total energy is for the case when the H atoms are on the same side, whereas they are alternating on the two different sides in the other case) and the two-layer results marked with circles (here, the lowest total energy is for the case when Al−O bonds form the bonds between the layers).

material is stoichiometric, suggest that stable structures of HAlO may occur for layers of HAlO. To study this proposal further, we considered theoretically extended HAlO systems consisting of either one or two layers of HAlO. We add that these calculations ignore interlayer interactions that can be very important and that, therefore, may modify our conclusions significantly, when included.

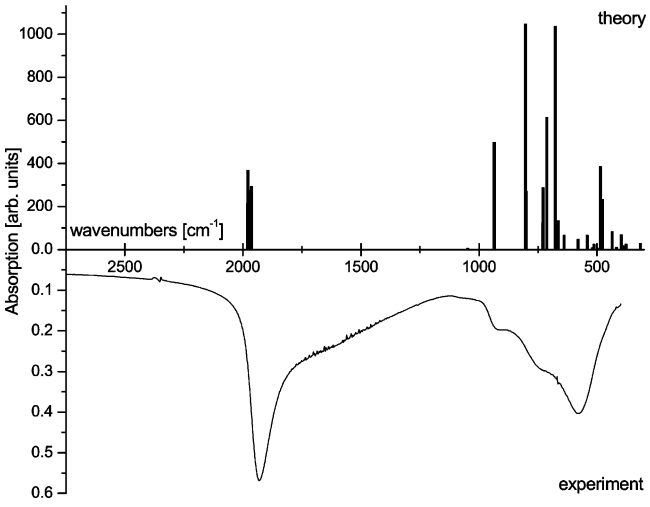

Figure 15. Comparison of calculated and experimental infrared spectra. The upper theoretical spectrum is calculated as the weighted average of the line spectra for the optimized structures of the $(HAlO)_n$ ($n = 2$, 3, 4, and 6) clusters. The experimental spectrum has been taken from a HAlO layer on a steel target with a reflection technique (angle 30°).

For a single layer of HAlO, one can imagine two highly symmetric cases, i.e., one where all H atoms are on one side of

TABLE 2: Properties of Two Interacting Clusters of n_1 and n_2 Units Giving in Total $n = n_1 + n_2$ Units[a]

n	n_1	n_2	$E_{tot}^{com}(n)$	$E_{tot}^{auf}(n)$	$E_{tot}^{ga}(n)$	$E_{tot}^{auf}(n_1) + E_{tot}^{auf}(n_2)$	$E_{tot}^{ga}(n_1) + E_{tot}^{ga}(n_2)$
5	2	3	−25.5948	−25.5948	−25.5948	−24.4301	−24.4301
6	2	4	−31.0983	−31.1353	−31.1483	−29.9168	−29.9168
7	3	4	−36.5535	−36.6566	−36.6632	−35.0518	−35.0518
12	4	8	−64.9534	−65.2908	−65.3370	−62.5828	−62.5956
17	8	9	−94.0379	−94.6440	−94.6602	−90.3529	−90.3828

[a] E_{tot}^{auf} or E_{tot}^{ga} gives the calculated total energy (in au) with either the Aufbau or the genetic-algorithms approach, respectively. $E_{tot}(n_1) + E_{tot}(n_2)$ gives results for the relaxed, noninteractions clusters, whereas $E_{tot}(n)$ gives results for the relaxed cluster of n units. Finally, $E_{tot}^{com}(n)$ gives results for the relaxed, combined clusters.

the layer, and one where every second H atom is above and every second H atom is below the AlO layer. These are shown in Figure 13. For the case that all H atoms are on the same side of the layer, the Al and O atoms form a layer with bond lengths of 3.33 au = 1.76 Å and 3.34 au =1.77 Å. Moreover, the hydrogen atoms are sitting on the outside of the layer bonded to the Al atoms with Al−H bond lengths of 3.21 au = 1.70 Å. The Al−O−Al bond angles are 85°−86° and 147°−152°.

Remarkably different things occur when the H atoms are sitting alternatingly on the two sides of the single AlO layer. Then we found that the layer split into several small parts all with the same kind of structure; that is, the H atoms are binding to the Al atoms with Al−H bond lengths around 3.08 au = 1.63 Å, whereas the Al−O bond lengths are around 3.40 au = 1.80 Å.

For the case of two layers of HAlO, we studied two cases, i.e., either the Al atoms of one layer were placed on top of the O atoms of the other layer, or they were placed on top of the Al atoms of the other layer. It turned out that the first situation was much more stable than the second one, which may not be surprising, and in the second case we find that the system breaks into small parts.

Finally, it is interesting to study the energy per unit for the finite clusters in comparison with that for the layers, shown in Figure 14. It is remarkable that the two-layer structure is not significantly more stable than the finite clusters. We believe that the systems prefer to have H atoms on some surface. However, since the surface area scales as $n^{2/3}$, the available area per H atom scales such as $n^{-1/3}$, meaning that, above a certain critical size, the finite $(HAlO)_n$ clusters will be less stable simply due to too little space for the H atoms on the surface. This effect is not found for the layers that per construction are infinite, but it suggests that there is a competition between clusters of HAlO and layers of HAlO, which may explain why the two different synthetic routes lead to different materials. It is not possible to determine directly the critical size of the finite $(HAlO)_n$ clusters above which they become unstable, but our results suggest that this size may be comparable to the largest clusters of the present study.

IV. Conclusions

HAlO, like other amorphous glasses, consists of many different structural entities. Experimental data (Al-NMR, IR) indicate that the aluminum atoms are coordinated by four, five, and six ligands (oxygen and hydrogen). Al−H as well as Al−H···Al entities, but no hydroxides, can be detected using infrared spectroscopy, in accordance with the results of the calculations.

In the present work we have determined the structure of HAlO clusters using two different unbiased approaches, i.e., the Aufbau and the genetic-algorithms approaches, in combination with a parametrized density-functional method for the calculation of electronic and energetic properties for a given structure. Moreover, for smaller clusters we also performed a large number of parameter-free density-functional calculations. The fact that all methods give very similar results makes us believe that the results are reliable. Also, the infrared spectra could be reproduced by the parameter-free density-functional calculations.

The optimized HAlO clusters were found to contain a core of AlO where, moreover, mainly heteroatomic bonds exist. The H atoms are found only on the surface of the core and are only bonded to Al. From the parameter-free density-functional calculations we could see that there is a strong energetic driving force for creating systems with Al−O bonds and, moreover, the clusters would prefer to have one Al−H bond per unit. The cluster with $n = 4$ has a very high symmetry. Moreover, the stability function shows that with increasing n the total energy per unit decreases monotonically. The combined clusters $n_1 + n_2$ are slightly more stable than the two isolated clusters of n_1 and n_2 units but significantly less stable than the optimized $n_1 + n_2$ cluster. We also found that infinite layered HAlO can be stable, in particular for a system consisting of two AlO layers bonded via Al−O bonds and with additional H atoms attached to the Al atoms. It turned out, however, that this system was only marginally more stable than the most stable cluster of our study.

These findings are in accord with our experimental results: We find that by thermal treatment of HAlO, the system loses hydrogen in the first place. The $(AlO)_n$ core is not affected in the first instance, but as it is electronically unsaturated, it decomposes by disproportionation to Al and Al_2O_3. Apart from the use of this metastability of the sytem in our experiments, we are also interested in the transient $(AlO)_n$ state, about which further theoretical and experimental work is underway.

Acknowledgment. This work was supported by the SFB 277 at the University of Saarland. The authors are very grateful to the Fonds der Chemischen Industrie for generous support.

Supporting Information Available: Results from the parameter-free density-functional calculations on the 50 isomers of $(HAlO)_n$ with $n = 1$, 2, 3, 4, and 6, including structural and energetic information. This material is available free of charge via the Internet at http://pubs.acs.org.

References and Notes

(1) Veith, M.; Andres, K.; Faber, S.; Blin, J.; Zimmer, M.; Wolf, Y.; Schnöckel, H.; Köppe, R.; Masi, R.; Hüfner, S. *Eur. J. Inorg. Chem.* **2003**, 4387.

(2) Veith, M.; Andres, K. *J. Metastable Nanocryst. Mater.* **2003**, *15*−*16*, 279.

(3) Liu, S. W.; Wehmschulte, R. J.; Burba, C. M. *J. Mater. Chem.* **2003**, *13*, 3107.

(4) Liu, S. W.; Fooken, J.; Burba, C. M.; Eastman, M. A.; Wehmschulte, R. J. *Chem. Mater.* **2003**, *15*, 2803.

(5) Dong, Y.; Springborg, M. In *Proceedings of 3rd International Conference "Computational Modeling and Simulation of Materials"*; Vincenzini, P., et al., Eds.; Techna Group Publishers: Faenza, Italy, 2004; p 167.

(6) Roszinski, H.; Dautel, R.; Zeil, W. *Z. Phys. Chem.* **1963**, *36*, 26.

(7) Go, E. P.; Tuermer, K.; Reutt-Robey, J. E. *Surf. Sci.* **1999**, *437*, 377.

(8) Porezag, D.; Frauenheim, Th.; Köhler, Th.; Seifert, G.; Kaschner, R. *Phys. Rev. B* **1995**, *51*, 12947.

(9) Seifert, G.; Schmidt, R. *New J. Chem.* **1992**, *16*, 1145.

(10) Seifert, G.; Porezag, D.; Frauenheim, Th. *Int. J. Quantum Chem.* **1996**, *58*, 185.

(11) Grigoryan, V. G.; Springborg, M. *Phys. Chem. Chem. Phys.* **2001**, *3*, 5125.

(12) Holland, J. H. *Adation in Natural Algorithms and Artifical systems*; University of Michigan Press: Ann Arbor, MI, 1975.

(13) Goldberg, D. E. *Genetic Algorithms in search, Optimization and Machine Learning*; Addison-Wesley: Reading, MA, 1989.
(14) Ahlrichs, R.; Bär, M.; Häser, M.; Horn, H.; Kölmel, C. *Chem. Phys. Lett.* **1989**, *162*, 165.
(15) Becke, A. D. *Phys. Rev. B* **1988**, *38*, 3098.
(16) Vosko, S. H.; Wilk, L.; Nusair, M. *Can. J. Phys.* **1980**, *58*, 1200.
(17) Perdew, J. P. *Phys. Rev. B* **1986**, *33*, 8822.
(18) Perdew, J. P. *Phys. Rev. B* **1986**, *34*, 7406.
(19) Schfer, A.; Horn, H.; Ahlrichs, R. *J. Chem. Phys.* **1992**, *97*, 2571.
(20) Eichkorn, K.; Treutler, O.; Öhm, H.; Häser, M.; Ahlrichs, R. *Chem. Phys. Lett.* **1995**, *240*, 283.
(21) Eichkorn, K.; Weigend, F.; Treutler, O.; Ahlrichs, R. *Theor. Chim. Acta* **1997**, *97*, 119.
(22) Hirota, F.; Tanimoto, M.; Tokiwa, H. *Chem. Phys. Lett.* **1993**, *208*, 115.
(23) Mason, M. R.; Smith, J. M.; Bott, S. G.; Barron, A. R. *J. Am. Chem. Soc.* **1993**, *115*, 4971.
(24) Wehmschulte, R. J.; Power, P. P. *J. Am. Chem. Soc.* **1997**, *119*, 8387.